

## The expected fluxes observed by STIX during low solar activity

M. Gryciuk<sup>a,b,\*</sup>, P. Podgórski<sup>a</sup>, S. Gburek<sup>a</sup>, T. Mrozek<sup>a,b</sup>, M. Siarkowski<sup>a</sup>, M. Steslicki<sup>a</sup>, J. Barylak<sup>a</sup>, A. Barylak<sup>a</sup>

<sup>a</sup> Solar Physics Division Space Research Centre, Polish Academy of Sciences, Bartycka 18A, 00-716 Warsaw, Poland

<sup>b</sup> Astronomical Institute, University of Wrocław, Kopernika 11, 51-622 Wrocław, Poland

### ARTICLE INFO

#### Keywords:

Solar instrumentation

X-rays2010 MSC:

00-01

99-00

### ABSTRACT

The Spectrometer Telescope for Imaging X-rays (STIX) is one of the instruments installed onboard Solar Orbiter mission which will be launched in February 2020. After 1.5 years of cruise phase it will start to gather scientific data from the orbit with perihelion distance about 0.28 au. It means that STIX will operate also during the next solar minimum. In the paper we estimate flux measured by the instrument during periods of low solar activity. For this purpose we used solar observations which were recorded by the Solar Photometer in X-rays (SphinX) during the last minimum of solar activity. The estimation was obtained for instruments overlapping energy range from 4 to 15 keV. Presented results indicate that STIX instrument will provide efficient imaging the solar emission even during low level of solar activity (B1 GOES class).

### 1. Introduction

Solar Orbiter (Müller et al., 2013), a European Space Agency's mission, will be launched with an Atlas V rocket from the Cape Canaveral in Florida in February 2020. Following launch, Solar Orbiter will begin its 1.5 year journey to the Sun. In order to reach its near-Sun orbit, the spacecraft will use a series of gravity assists from Venus and the Earth, in essence, using them to catapult itself towards the Sun. The Spectrometer/Telescope for Imaging X-rays (STIX: (Krucker et al., 2016)) is one of the 10 instruments that are part of the scientific payload for the Solar Orbiter mission. STIX will provide imaging spectroscopy of thermal and non-thermal solar X-ray emission from 4 to 150 keV. It applies a Fourier-imaging technique using a set of tungsten grids in front of 30 pixelated CdTe detectors. Although STIX instrument is designed to observe flares events, we decided to estimate flux measured by the instrument during period of low solar activity. For this purpose we used solar observations which were recorded by the Solar Photometer in X-rays (SphinX: (Sylwester et al., 2008; Gburek et al., 2013; Gryciuk et al., 2017)), instrument designed to observe soft X-ray (SXR) solar emission in the energy range between 1 keV and 15 keV with the resolution better than 0.5 keV. The SphinX operated from February until November 2009 aboard CORONAS-Photon satellite, during the phase of exceptionally low minimum of solar activity.

### 2. Data and calculations

In order to evaluate expected flux observed by STIX detectors during low solar activity we selected a time period in which SphinX spectrophotometer has recorded X-ray emission of B1 class intensity in standard GOES classification. This emission comes from quiet Sun and two small active regions as well (NOAA numbers 11028 and 11029). One of the AR's (11029) was highly active and produced in total 73 flares (Gilchrist et al., 2012). Fig. 1 shows SphinX observed spectrum integrated within selected time period from 11:20 UT to 11:50 UT on 25.10.2009. The time period was selected to have long observational data with constant level of SXR emission.

In the next step we used SphinX Detector Response Matrix (DRM) to reconstruct input photon flux. The SphinX DRM has been determined based on results of extensive preflight instrument calibration performed at the Physikalisch-Technische Bundesanstalt (PTB, Berlin, Germany) calibration facility using the BESSY II synchrotron as a primary source standard. The DRM is described in SphinX user guide document available on the webpage of the Solar Physics Division, Space Research Centre of Polish Academy of Sciences (SRC-PAS).<sup>1</sup>

The reconstructed solar spectrum shown in Fig. 2 was used as an input data for our estimation. A simple exponential fit (blue) to the observed spectrum was used to estimate the flux over entire considered energy range up to 15 keV. Green line indicates the spectrum model corrected for STIX distance to the Sun (0.28 au at perihelion). This

\* Corresponding author. Solar Physics Division Space Research Centre, Polish Academy of Sciences, Bartycka 18A, 00-716 Warsaw, Poland.

E-mail address: [mg@cbk.pan.wroc.pl](mailto:mg@cbk.pan.wroc.pl) (M. Gryciuk).

<sup>1</sup> [http://156.17.94.1/sphinx\\_l1\\_catalogue/CALIB\\_SOFT\\_GUIDE/SphinX\\_user\\_guide\\_v1\\_1.pdf](http://156.17.94.1/sphinx_l1_catalogue/CALIB_SOFT_GUIDE/SphinX_user_guide_v1_1.pdf).

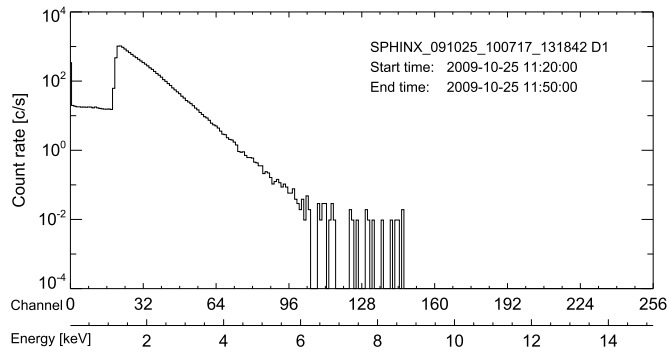


Fig. 1. A SphinX 1.2–15 keV spectrum integrated during 0.5 h of observations.

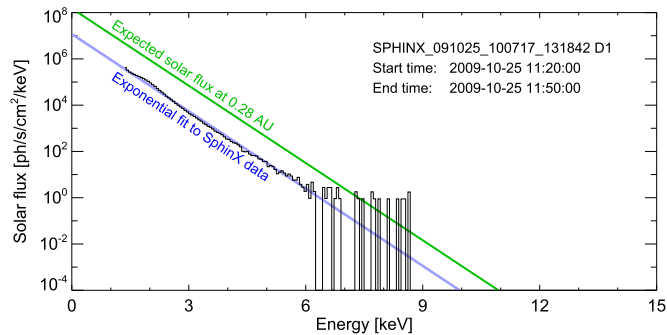


Fig. 2. The reconstructed solar flux with exponential model overplotted. Green line indicates the spectrum model corrected for STIX distance to the Sun. (For interpretation of the references to colour in this figure legend, the reader is referred to the Web version of this article.)

(green) flux is a STIX input flux in our estimation.

To obtain the flux reaching the STIX detectors we took into account STIX entrance filters transmission shown in Fig. 3. Resultant filter transmission is determined by two Be filters of total thickness of 3 mm and 5  $\mu\text{m}$  layer of Solar Black coating. Additionally the input flux is reduced by the grids assemblies. We assumed mean value of all grids transmission equal to 26.5%. Expected solar flux after passing the entrance filters and grids is shown in Fig. 4 as a black curve.

To estimate the STIX count rate for this input flux, we used STIX DRM. This DRM was modelled using Geant4 toolkit in energy range up to 15 keV.

By the matrix multiplication of the STIX DRM and input flux we obtained STIX response in units of  $\text{counts/s/cm}^2/\text{keV}$  as it would be observed in 256 energy bins covering energy range from 0 to 15 keV. The result is shown in Fig. 5. The vertical dotted line in this plot indicates STIX detection threshold at 4 keV.

In the last step we rebinned the obtained result to reflect real widths of STIX energy channels. Within energy range from 4 to 15 keV, these

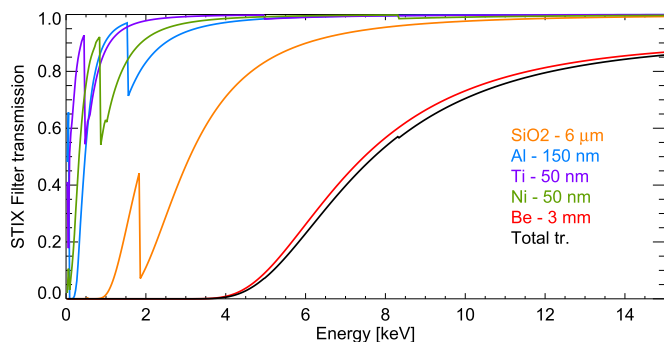


Fig. 3. STIX entrance filters transmission. Black line presents total transition.

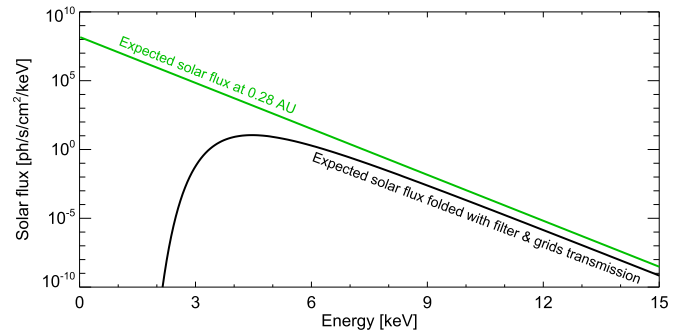


Fig. 4. Expected solar flux after passing the STIX entrance filters and grids.

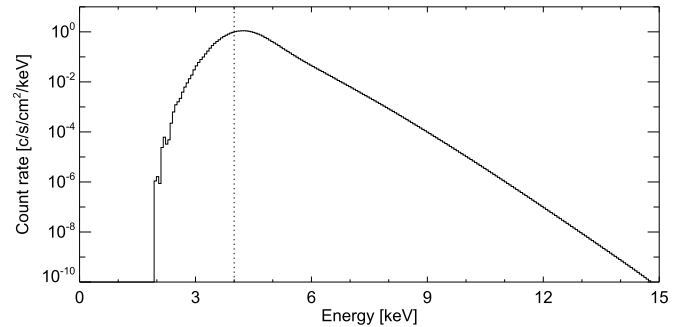


Fig. 5. Solar spectrum as observed by STIX. The vertical dotted line indicates instrumental energy threshold (4 keV).

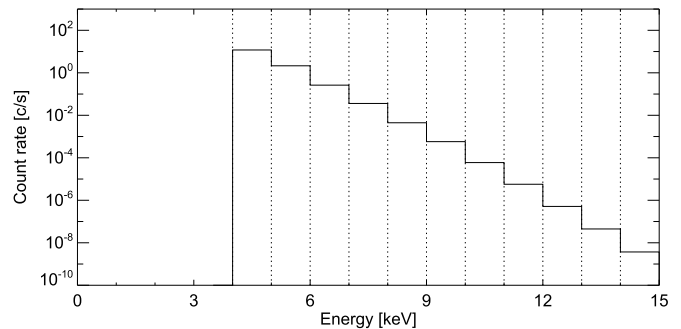


Fig. 6. Expected STIX spectrum in individual energy bins for input solar flux of GOES B1 class intensity.

channels have equal widths of 1 keV. Additionally a total area of single detector ( $0.81 \text{ cm}^2$ ) was taken into account to express the count rates in c/s. Fig. 6 shows expected count rates in individual STIX energy bins for input solar flux of GOES B1 class intensity.

### 3. Results and conclusions

We have estimated the expected flux which would be observed by the STIX instrument during periods of low solar activity (B1 GOES class level). Obtained results suggests that STIX will be able to register about 11 counts per second in a single detector in energy range from 4–15 keV. Due to low flux intensities and their spectrum slope inclinations, STIX would record the counts in a first energy bins (up to few keV). We have repeated the same estimation process for higher activity - B4 class solar flare. In this case, the estimated output count rate increased to about 550 counts per second in the same energy range.

The actual background countrate for STIX will be measured once instruments start operating. But the estimated background counts for STIX is equal to  $0.2 \text{ counts/s/cm}^2/\text{keV}$  in the analysed energy range (Casadei et al., 2017).

Having the above into account we conclude that STIX will provide useful, efficient imaging of active regions in solar corona in relative short integration times even during low solar activity (B class and higher).

### Acknowledgements

This work was supported by the Polish National Science Centre grants number 2015/19/B/ST9/02826 and 2015/17/N/ST9/03555.

### References

- Casadei, D., Jeffrey, N.L.S., Kontar, E.P., 2017. Measuring x-ray anisotropy in solar flares. prospective stereoscopic capabilities of stix and misofa. *Astron. Astrophys.* 606 <http://dx.doi.org/10.1051/0004-6361/201730629>. A2.
- Gburek, S., Sylwester, J., Kowalinski, M., Bakala, J., Kordylewski, Z., Podgorski, P., Plocieniak, S., Siarkowski, M., Sylwester, B., Trzebinski, W., Kuzin, S.V., Pertsov, A.A., Kotov, Y.D., Farnik, F., Reale, F., Phillips, K.J.H., 2013. Sphinx: the solar photometer in x-rays. *Sol. Phys.* 283, 631–649. <http://dx.doi.org/10.1007/s11207-012-0201-8>.
- Gilchrist, S.A., Wheatland, M.S., Leka, K.D., 2012. The free energy of noaa solar active region ar 11029. *Sol. Phys.* 276, 133–160. <http://dx.doi.org/10.1007/s11207-011-9878-3>.
- Gryciuk, M., Siarkowski, M., Sylwester, J., Gburek, S., Podgorski, P., Kepa, A., Sylwester, B., Mrozek, T., 2017. Flare characteristics from x-ray light curves. *Sol. Phys.* 292, 77–95. <http://dx.doi.org/10.1007/s11207-017-1101-8>.
- Krucker, S., Bednarzik, M., Grimm, O., Hurford, G.J., Limousin, O., Meuris, A., Orleński, P., Seweryn, K., Skup, K.R., 2016. The spectrometer/telescope for imaging x-rays on solar orbiter: flight design, challenges and trade-offs. *Nucl. Instrum. Meth. Phys. Res.* 824, 626–629. <http://dx.doi.org/10.1016/j.nima.2015.08.045>.
- Müller, D., Marsden, R.G., St Cyr, O.C., Gilbert, H.R., 2013. Solar orbiter. exploring the sun-heliosphere connection. *Sol. Phys.* 285, 25–70. <http://dx.doi.org/10.1007/s11207-012-0085-7>.
- Sylwester, J., Kuzin, S., Kotov, Y.D., Farnik, F., Reale, F., 2008. Sphinx: a fast solar photometer in x-rays. *J. Astrophys. Astron.* 29, 339–343. <http://dx.doi.org/10.1007/s12036-008-0044-8>.